Karolinska Institutet

http://openarchive.ki.se

This is a Peer Reviewed Published version of the following article, accepted for publication in Journal of nuclear medicine.

2012-10-02

HER2-positive tumors imaged within 1 hour using a site-specifically 11C-labeled sel-tagged affibody molecule

Wållberg, Helena; Grafström, Jonas; Cheng, Qing; Lu, Li; Ahlzén, Hanna-Stina; Samén, Erik; Thorell, Jan-Olov; Johansson, Katarina; Dunås, Finn; Olofsson, Maria Hägg; Stone-Elander, Sharon; Arnér, Elias S J; Ståhl, Stefan

J Nucl Med. 2012 Sep;53(9):1446-53.
http://doi.org/10.2967/jnumed.111.102194
http://hdl.handle.net/10616/41230

If not otherwise stated by the Publisher's Terms and conditions, the manuscript is deposited under the terms of the Creative Commons Attribution-NonCommercial-NoDerivatives License (http://creativecommons.org/licenses/by-nc-nd/4.0/), which permits non-commercial re-use, distribution, and reproduction in any medium, provided the original work is properly cited, and is not altered, transformed, or built upon in any way.

HER2-Positive Tumors Imaged Within 1 Hour Using a Site-Specifically ^{11}C-Labeled Sel-Tagged Affibody Molecule

Helena Wållberg[1], Jonas Grafström[2], Qing Cheng[3], Li Lu[2,4], Hanna-Stina Martinsson Ahlzén[3], Erik Samén[2,5], Jan-Olov Thorell[2,5], Katarina Johansson[3], Finn Dunås[6], Maria Hägg Olofsson[7], Sharon Stone-Elander[2,5], Elias S.J. Arnér[3], and Stefan Ståhl[1]

[1]Division of Molecular Biotechnology, School of Biotechnology, AlbaNova University Center, Royal Institute of Technology, Stockholm, Sweden; [2]Department of Clinical Neuroscience, Karolinska Institutet, Stockholm, Sweden; [3]Division of Biochemistry, Department of Medical Biochemistry and Biophysics, Karolinska Institutet, Stockholm, Sweden; [4]Karoliniska Experimental Research and Imaging Center, Karolinska University Hospital, Solna, Sweden; [5]Department of Neuroradiology, Karolinska University Hospital, Solna, Sweden; [6]Affibody AB, Solna, Sweden; and [7]Department of Oncology-Pathology, Karolinska Institutet, Stockholm, Sweden

A rapid, reliable method for distinguishing tumors or metastases that overexpress human epidermal growth factor receptor 2 (HER2) from those that do not is highly desired for individualizing therapy and predicting prognoses. In vivo imaging methods are available but not yet in clinical practice; new methodologies improving speed, sensitivity, and specificity are required. **Methods:** A HER2-binding Affibody molecule, $Z_{HER2:342}$, was recombinantly fused with a C-terminal selenocysteine-containing tetrapeptide Sel-tag, allowing site-specific labeling with either ^{11}C or ^{68}Ga, followed by biodistribution studies with small-animal PET. Dosimetry data for the 2 radiotracers were compared. Imaging of HER2-expressing human tumor xenografts was performed using the ^{11}C-labeled Affibody molecule. **Results:** Both the ^{11}C- and ^{68}Ga-labeled tracers initially cleared rapidly from the blood, followed by a slower decrease to 4–5 percentage injected dose per gram of tissue at 1 h. Final retention in the kidneys was much lower (>5-fold) for the ^{11}C-labeled protein, and its overall absorbed dose was considerably lower. ^{11}C-$Z_{HER2:342}$ showed excellent tumor-targeting capability, with almost 10 percentage injected dose per gram of tissue in HER2-expressing tumors within 1 h. Specificity was demonstrated by preblocking binding sites with excess ligand, yielding significantly reduced radiotracer uptake ($P = 0.002$), comparable to uptake in tumors with low HER2 expression. **Conclusion:** To our knowledge, the Sel-tagging technique is the first that enables site-specific ^{11}C-radiolabeling of proteins. Here we present the finding that, in a favorable combination between radionuclide half-life and in vivo pharmacokinetics of the Affibody molecules, ^{11}C-labeled Sel-tagged $Z_{HER2:342}$ can successfully be used for rapid and repeated PET studies of HER2 expression in tumors.

Key Words: Affibody molecule; Sel-tag; ^{11}C; selenium; positron emission tomography

J Nucl Med 2012; 53:1446–1453
DOI: 10.2967/jnumed.111.102194

Overexpression of the human epidermal growth factor receptor 2 (HER2), found in about 20%–30% of breast cancers, is associated with poor prognosis, and HER2 is the molecular target for effective but expensive monoclonal antibody drugs such as trastuzumab (Herceptin; Roche) (*1*). Determination of the expression levels of HER2 is therefore important for predicting prognosis and for patient stratification for treatment. Currently, expression levels are mainly determined using biopsies for molecular assays such as in situ hybridization (*2*). These procedures are, however, invasive, are difficult to perform repeatedly, and risk missing overexpressing tissue due to sampling errors. Therefore, the radionuclide-based in vivo molecular imaging of HER2, primarily using polypeptide probes, is rapidly expanding, aiming for personalized medicine with image-and-treat strategies (*3–6*). Speed, sensitivity, and specificity are necessary for implementation in clinical routines.

Comparing nuclear medicine imaging techniques, PET has better spatial resolution, higher sensitivity, and more accurate quantification than SPECT. With recent radiolabeling advances, the feasibility of using polypeptides for PET has increased (*4,7,8*). Although ^{18}F (energy maximum of emitted positron [E_{max}], 0.635 MeV; half-life [$t_{1/2}$], 109.8 min; 97% β^+-decay) is the PET nuclide most used clinically, the shorter-lived ^{11}C (E_{max}, 0.96 MeV; $t_{1/2}$, 20.4 min; 100% β^+-decay) is also widely used in PET molecular imaging and in clinical evaluations of a range of cancers (*9,10*). Its relatively low positron energy is suitable for high-resolution imaging. Its short half-life and complete decay by positron emission give lower radiation doses and allow same-day imaging and repeated investigations with either the same or different radiotracers within a few hours, all of which are desirable options for longitudinal therapy monitoring. The in vivo observation of ^{11}C-labeled tracers is limited to about 60–80 min, so they must clear rapidly from nonspecific compartments for high-contrast imaging of molecular targets. Also, the labeling method must be rapid and, for many proteins, avoid denaturing conditions to maintain protein integ-

Received Dec. 20, 2011; revision accepted Apr. 30, 2012.
For correspondence or reprints contact: Stefan Ståhl, Division of Molecular Biotechnology, School of Biotechnology, AlbaNova University Center, Royal Institute of Technology (KTH), SE-106 91 Stockholm, Sweden.
E-mail: stefan.stahl@biotech.kth.se
Published online Aug. 7, 2012.
COPYRIGHT © 2012 by the Society of Nuclear Medicine and Molecular Imaging, Inc.

rity and target-binding features. The only reported way to site-specifically label proteins with ^{11}C uses a Sel-tag, a small tetrapeptide motif containing a selenocysteine residue (denoted Sec or U) in a C-terminal -Gly-Cys-Sec-Gly sequence (*11,12*). In its oxidized state, the Cys-Sec pair forms an inert selenenylsulfide. When it is reduced, the Sec becomes exposed as a highly reactive nucleophile that can rapidly react with electrophiles such as ^{11}C-methyl iodide (CH_3I) for ^{11}C-labeling (*11,12*). In this study, we have investigated the use of this technique to ^{11}C-label an Affibody molecule (Affibody AB) for HER2 imaging in vivo.

Affibody molecules are highly stable scaffold proteins derived from staphylococcal protein A (*13*). By randomizing 13 surface residues, large libraries of affinity proteins have been created, from which binders to several different targets have been selected by various methods (*14*). Their small size (58 residues, 6.5 kDa), high thermal and pH stability, cost-efficient production, and potentially high target-binding affinity and specificity make them attractive candidates for radionuclide-based molecular imaging (*15*). The best-characterized Affibody molecule to date has picomolar affinity to HER2 (*16*) and has been labeled with, for example, ^{111}In, ^{99m}Tc, ^{68}Ga, and ^{18}F and successfully used in preclinical (*17*) and clinical (*18*) molecular imaging. Because Affibody molecules display rapid pharmacokinetics, are quickly cleared from the circulatory system, and have a size well below the molecular weight limit for glomerular filtration, we reasoned that they might be appropriately labeled with even shorter-lived radionuclides such as ^{11}C.

The HER2 binder $Z_{HER2:342}$ (*16*) was used here for ^{11}C-labeling, and an epidermal growth factor receptor (EGFR)–targeting Affibody molecule, $Z_{EGFR:2377}$ (*19*), was also included to demonstrate the general applicability of the tagging technique with maintained specificity in target binding. To compare the pharmacokinetics of the ^{11}C-labeled tracer with that of previous probes (*18,20*), $Z_{HER2:342}$-ST was alternatively labeled with ^{68}Ga (E_{max}, 1.9 MeV; $t_{1/2}$, 68 min; 89% β^+-decay), a generator-produced positron emitter that is increasingly being used in nuclear medicine. We present results that collectively suggest that ^{11}C-labeled Sel-tagged Affibody molecules may prove highly useful in tumor receptor–based PET, here exemplified with HER2-expressing tumors.

MATERIALS AND METHODS

Protein Ligand Production

$Z_{EGFR:2377}$ (*19*) and $Z_{HER2:342}$ (*16*) were recombinantly fused with a C-terminal Sel-tag and produced using the methods described by Cheng et al. (*11*). For a detailed description, see the supplemental materials (available online only at http://jnm.snmjournals.org). $Z_{HER2:342}$, intended for in vivo studies, was produced with and without an N-terminal His_6-tag, because His_6-tags may cause undesirable elevated liver uptake (*21,22*). The phenylarsine oxide Sepharose (GE Healthcare) purification of Sel-tagged proteins (*11,12*) was not used here, to avoid in vivo usage of proteins passed over arsenic-based columns. Consequently, the proteins used were a mixture of UGA (opal stop codon)-truncated -GC tagged and Sec-containing full-length -GCUG variants, where U is Sec (*11,12*). A schematic representation of the Affibody molecule with the C-terminal Sel-tag and its reactions as used here is depicted in Figure 1.

Fluorescent Labeling of Sel-Tagged Proteins

His_6-$Z_{EGFR:2377}$-ST, His_6-$Z_{HER2:342}$-ST, and $Z_{HER2:342}$-ST were site-specifically labeled at the Sec residue with 5-IAF (Invitrogen). A description of the procedure is provided in the supplemental materials.

Cell-Binding Analysis Using Fluorescence-Activated Cell Sorting

To verify retained specific binding of the Affibody molecules to their respective targets after Sel-tagging and labeling with 5-IAF, the binding of IAF-labeled His_6-$Z_{EGFR:2377}$-ST, His_6-$Z_{HER2:342}$-ST, and $Z_{HER2:342}$-ST was analyzed using fluorescence-activated cell sorting. A detailed description of cell lines, culture conditions, and the procedure is provided in the supplemental materials.

Radiolabeling of $Z_{HER2:342}$-ST

Labeling with ^{11}C. ^{11}C-methane was produced by the ^{14}N(p,α)^{11}C reaction using a PETtrace cyclotron (GE Healthcare) and was converted to ^{11}C-CH_3I in a gas phase reaction (*23*) using a Tracerlab FX C Pro synthesis module (GE Healthcare). The

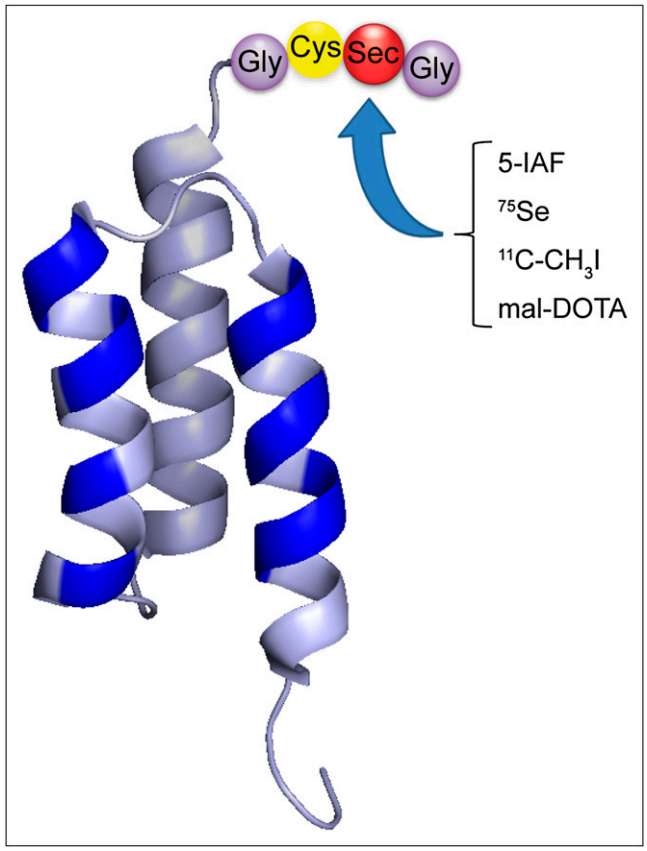

FIGURE 1. Overview of Sel-tagged Affibody format and its applications. Schematic representation of Affibody molecule and C-terminal Sel-tag. Randomized positions in binding site of Affibody scaffold are indicated in blue, and Sel-tag is indicated in 3-letter code. Sel-tag was used here for labeling with fluorescent 5-IAF, labeling with ^{75}Se and ^{11}C, and conjugation with maleimide-DOTA for labeling with ^{68}Ga.

labeling precursor was trapped in dimethylsulfoxide (0.2 mL) at room temperature. Lyophilized $Z_{HER2:342}$-ST (250 μg, 33 nmol) was dissolved in 150 μL of phosphate-buffered saline and reduced by the addition of dithiothreitol to a final concentration of 2 mM and incubated for 30 min at 35°C. An aliquot of the ^{11}C-CH_3I–dimethylsulfoxide solution (150 μL) was added to the reaction mixture. After incubation at 35°C for 20–25 min, the labeled protein was purified by size-exclusion chromatography using a NAP-5 column (GE Healthcare) preequilibrated with phosphate-buffered saline. The radiochemical purity and identity were assessed by radio–high-performance liquid chromatography (HPLC) using ultraviolet (210 nm) and radioactivity detectors in series and a Superdex Peptide 10/300 GL column (GE Healthcare) eluted with phosphate-buffered saline.

Labeling with ^{68}Ga. For labeling with ^{68}Ga, $Z_{HER2:342}$-ST was conjugated with the macrocyclic chelator maleimido-monoamide-DOTA (Macrocyclics) by targeting the Sel-tag, in analogy to the previously described method using Cys-containing proteins (*24*). The conjugate was purified by reversed-phase HPLC, using a Reprosil Gold 300 C18 (5 μm, 250 × 10 mm) column, before analysis by liquid chromatography–mass spectrometry and subsequent lyophilization of the conjugate.

The elution, purification, and preconcentration of ^{68}Ga from the ^{68}Ge/^{68}Ga generator (The Open Joint Stock Company Isotope) were performed as previously described (*25*). The labeling was performed similarly to the method of Tolmachev et al. (*20*). Lyophilized $Z_{HER2:342}$-ST-DOTA (50 μg, 6.6 nmol) was dissolved in the ^{68}Ga concentrate (150–200 μL), and pH was adjusted to 3.5 using sodium acetate (1.25 M). The labeling mixture was incubated at 90°C for 15 min before purification on NAP-5 and HPLC analysis.

The stability of ^{68}Ga-$Z_{HER2:342}$-ST-DOTA was assessed by incubation in a 500-fold molar excess of ethylenediaminetetraacetic acid (EDTA) at room temperature for 60 min before analysis by radio–instant thin-layer chromatography eluted with 0.2 M citric acid. As a control, ^{68}Ga-$Z_{HER2:342}$-ST-DOTA was incubated in water and analyzed in parallel. Furthermore, the stability of ^{68}Ga-$Z_{HER2:342}$-ST-DOTA in plasma was investigated by incubating the protein in murine plasma at 37°C for 1 h and subsequently analyzed by radio–sodium dodecyl sulfate polyacrylamide gel electrophoresis.

In Vivo Small-Animal PET Studies

Experiments were performed in accordance with national legislation on laboratory animals' protection and were approved by the local ethics committee for animal research. The in vivo characterizations of the radiotracers were studied using female severe combined immunodeficiency mice without or with SKOV-3 or A431 xenografts (high or low levels of HER2, respectively). Mice were inoculated in the right shoulder by subcutaneous injection of 10^7 cells, and the SKOV-3 or A431 xenografts were allowed to grow for 6 or 2 wk, respectively. The average size of the tumors at the time of the experiment was 121 ± 35 mm^3 for SKOV-3 and 216 ± 256 mm^3 for A431 tumors. The mice were anesthetized with isoflurane (5% initially, and then 1.5% during scans) using Microflex nonrebreather masks (Euthanex Corp.) and kept on heating beds (37°C) during experiments. An aliquot of the radiotracer was diluted with saline to 200 μL for intravenous (tail vein) injections. Dynamic PET images were acquired using a microPET Focus120 (CTI Concorde Microsystems), processed with microPET Manager (CTI Concorde Microsystems) and evaluated using Inveon Research Workplace (Siemens Medical Solutions) software. Data were collected every second from the time of injection for 1 h and corrected for randoms, dead time, and decay. Images were reconstructed by standard 2-dimensional filtered backprojection using a ramp filter and framed to 6 × 10 s, 10 × 1 min, and 8 × 5 min.

To determine the temporal changes of tracer concentrations, regions of interest based on postmortem measurements of the tumor dimensions were drawn on the images. Radioactivity concentrations (Bq/mL) were calculated by calibrating against a phantom with a known concentration of radioactivity. Assuming a tissue density of 1 g/mL, the radioactivity concentrations were divided by the administered activity to obtain a percentage injected dose per gram of tissue (%ID/g) derived from regions of interest. In comparisons between different individuals, normalization for body weight was performed.

Comparative Biodistribution of ^{11}C- and ^{68}Ga-Labeled Sel-Tagged Affibody Molecules. Biodistributions of ^{11}C-$Z_{HER2:342}$-ST and ^{68}Ga-$Z_{HER2:342}$-ST-DOTA were compared in severe combined immunodeficiency mice (n = 2). Mice were injected intravenously with ^{11}C-$Z_{HER2:342}$-ST (3–4 MBq, 20 μg [2.7 nmol]) and imaged for 1 h. After complete decay of ^{11}C (>10 half-lives), the same mice were injected intravenously with ^{68}Ga-$Z_{HER2:342}$-ST-DOTA (7–8 MBq, 3 μg [0.4 nmol]) and imaged for an additional hour.

Dosimetry Calculations. The dose ratio was estimated using the effective half-lives based on the time–activity curves generated for the regions of interest in the whole body, liver, and kidneys after tracer administration. The dose ratio was then combined with values of absorbed dose per unit-cumulated activity tabulated by MIRD pamphlet 11 (*26*). Backscattered radiation was omitted.

Tumor-Targeting Studies. The tumor-targeting capability of ^{11}C-$Z_{HER2:342}$-ST was investigated in mice with SKOV-3 tumors. Mice (n = 8) were injected intravenously with radiotracer (4–8 MBq, 6–26 μg, 0.80–3.4; average, 1.9 nmol) and imaged for 1 h. To determine specificity of tumor uptake, the same mice were subcutaneously or intravenously injected with a blocking dose (250 μg, 33 nmol) of nonradioactive $Z_{HER2:342}$-ST under maintained anesthesia and then allowed to recover. After approximately 1 h, mice were sedated, injected with ^{11}C-$Z_{HER2:342}$-ST, and imaged for 1 h. Mice with A431 xenografts (low HER2 expression levels) (n = 4) were injected intravenously with ^{11}C-$Z_{HER2:342}$-ST and imaged.

After completed imaging, the mice were euthanized by cervical dislocation under continued anesthesia, after which urine, blood, and tissue samples were immediately collected. The tumors were dissected and snap-frozen for subsequent analysis of HER2 expression by immunohistochemistry.

Radiotracer Stability. To examine the protein degradation and excretion of ^{11}C-labeled radiometabolites, the urine and plasma samples collected after death were precipitated with ice-cold acetone and the insoluble and soluble fractions separated (*27*). Briefly, 1 mL of ice-cold acetone was added to the sample (50–100 μL), stirred in a vortex mixer, incubated at −20°C for 20 min, and centrifuged. The supernatant and pellet with low- and high-molecular-weight compounds, respectively, were separated, and radioactivity was measured.

Immunohistochemistry

The monoclonal mouse anti-HER2 antibody 2F5 that was used as the primary antibody for the detection of HER2 by immunohistochemistry was kindly provided by Dr. Johan Rockberg. Excised tumors were fixed in 2% formalin, and staining was performed as previously described (*28*).

Statistical Analysis

Data are expressed as mean values with 95% confidence intervals using a Student *t* distribution. To determine significant differences in tumor uptake between baseline scans and after blocking with nonlabeled tracer in the same animals, data were analyzed by a paired 2-tailed *t* test. For comparison of uptake in different tumor models, an unpaired 2-tailed *t* test was used, with equal variances not assumed. Differences were considered significant if the *P* value was less than 0.05.

RESULTS

Receptor Binding of Sel-Tagged Affibody Molecules

Sel-tagged Affibody molecules were labeled with 5-IAF for cell-binding studies by flow cytometry (Fig. 2). The HER2-binding Affibody molecules clearly bound to HER2-overexpressing SKOV-3 and MDA-MB-453 cells, whereas only low fluorescence was observed with A431 cells having low HER2 expression levels (Fig. 2, top). The EGFR-binding Affibody molecule bound to EGFR-expressing A431 cells but not SKOV-3 or MDA-MB-453 cells (Fig. 2, bottom). Specificity was also demonstrated by blocking with a 10-fold excess of nonlabeled protein, which significantly reduced the cell-associated fluorescence (Fig. 2). Thus, neither the Sel-tag nor its labeling with 5-IAF disrupted the previously well-characterized specific high-affinity receptor–binding capability of these Affibody molecules (*16,19*). These results encouraged us to further investigate the efficacy of Sel-tagged Affibody molecules for receptor-targeted imaging in vivo.

Sel-Tag Mediated Radiolabeling with ^{11}C and ^{68}Ga

$Z_{HER2:342}$-ST was site-specifically labeled with ^{11}C and ^{68}Ga for subsequent characterization in vivo. Covalent labeling with ^{11}C was achieved by reacting the reduced Sel-tag with ^{11}C-CH_3I. Procedures for radiolabeling and purification over the NAP-5 column were completed within 40–45 min from the end of bombardment and 30 min (~1.5 half-lives) from the addition of ^{11}C-CH_3I to the reduced protein. The yields (decay-corrected) and specific activities were 5%–15% and 10–30 GBq/μmol, respectively. This specific activity is consistent with the truncated and unlabeled protein still being present in the isolated product but is well within levels previously determined necessary for imaging tumors with high HER2 expression (*29*). The radiochemical purity was greater than 97%, according to radio-HPLC analysis.

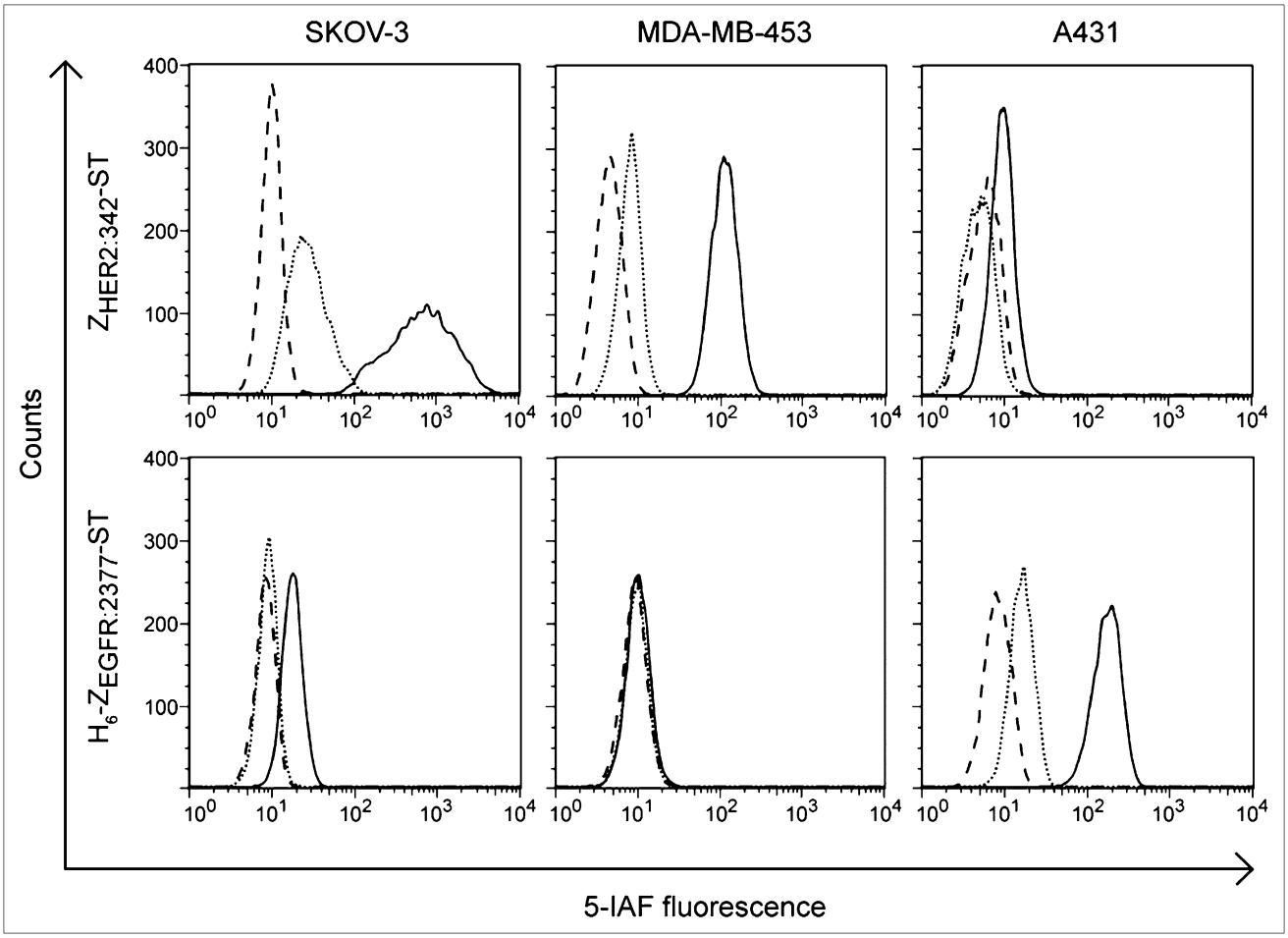

FIGURE 2. Binding and specificity analysis of Sel-tagged, fluorescently labeled Affibody molecules binding to SKOV-3 cells, MDA-MB-453 cells, and A431 cells. Figure shows HER2-binding $Z_{HER2:342}$-ST and EGFR-binding H6-$Z_{EGFR:2377}$-ST without blocking (solid line) and with blocking with 10 times excess of nonlabeled binder (dotted line) and control cells without staining (dashed line).

For labeling with ^{68}Ga, the Sel-tag was reacted with maleimide-DOTA, for subsequent DOTA coordination of the radiometal. The nonoptimized yield and specific activities of the ^{68}Ga-labeled protein were 31% and 14 GBq/μmol, respectively, and the radiochemical purity was 94% after NAP-5 elution.

^{68}Ga-$Z_{HER2:342}$-ST-DOTA was subjected to EDTA challenge and incubation in murine plasma in vitro. Radioactivity distribution on instant thin-layer chromatography after EDTA challenge was similar to a control sample in which ^{68}Ga-$Z_{HER2:342}$-ST-DOTA had been incubated in water, with 90%–95% of radioactivity still associated with the Affibody molecule (data not shown). Similarly, the only radioactive peak observed on sodium dodecyl sulfate polyacrylamide gel electrophoresis after incubation in plasma corresponded to intact Affibody molecule, indicating that the radiometal conjugate was stable over time and that transchelation to serum proteins or EDTA could be disregarded.

In Vivo Characterization

Comparative Biodistribution of ^{11}C- and ^{68}Ga-Labeled Affibody Molecules. Representative PET images summed for 0–60 min after injection of the ^{11}C- and ^{68}Ga-labeled tracers are shown in Figure 3A. Blood radioactivity showed an initial rapid distribution phase, with radioactivity concentrations subsequently decreasing after the first 30 min, with a half-life of 2 and 6 h for the ^{11}C- and ^{68}Ga-labeled tracers, respectively (Fig. 3B). One hour after injection, the radioactivity concentration in blood was 3.9 %ID/g and 4.9 %ID/g, respectively. The largest tissue concentrations of ^{11}C, in the kidneys and liver, were confirmed by ex vivo measurements, which also revealed concentrations in the pancreas and lung that were comparable to those in the liver (Supplemental Fig. 1).

After the initial distribution to the liver, the radioactivity concentration declined to about twice that in the blood at 60 min. After 30 min, the ^{68}Ga radioactivity cleared from the liver, with a half-life of 7.4 h, whereas ^{11}C slightly increased (0.4 %ID/g) during the last 30 min of the scan, possibly indicating hepatic metabolism of the radiotracer. In agreement with previous studies of Affibody molecules (*21,30*), the radioactivity was primarily excreted via the kidneys. Residualizing ^{68}Ga accumulated in the kidneys, increasing by 8 %ID/g during the last 30 min of the scan, probably because of the reabsorption of the tracer in proximal tubules and subsequent intracellular trapping of the radiometal. In contrast, the nonresidualizing ^{11}C was more efficiently cleared, with a $t_{1/2}$ of 14 min between 10 and 22 min and more slowly thereafter ($t_{1/2}$, 40 min after 30 min). One hour after injection, the concentration of radioactivity in the kidneys was 5-fold higher for ^{68}Ga than for ^{11}C (Fig. 3B). The dose ratio was 4.9, that is, the absorbed dose from ^{68}Ga is approximately 5 times that from ^{11}C.

^{11}C Radiometabolite Studies. Analyses of samples taken after death indicated that most of the radioactivity in plasma and whole blood was acetone-insoluble, high-molecular-weight compounds (≈75% at 40 min), whereas that in the urine was almost exclusively (>95%) acetone-soluble, lower-molecular-weight nonprotein compounds. This finding was supported by liquid chromatography–mass spectrometry analysis of the collected urine samples, in which no intact Affibody molecule was detected. Analyses of the ^{11}C radioactivity in the entire mouse body consistently indicated a decrease of 10%–15% of the injected dose throughout the PET scan, interpreted as loss of volatile radiometabolites through exhalation.

Rapid HER2 Imaging in Xenograft-Bearing Mice. The tumor-targeting capability of ^{11}C-$Z_{HER2:342}$-ST was investigated in mice carrying SKOV-3 xenografts. The specificity of tumor uptake was investigated by blocking experiments performed 2–3 h later in the same animals or by imaging A431 xenografts, which express lower levels of HER2.

Two representative PET images, summed for 10–60 min, clearly show the SKOV-3 tumor in the baseline scans (Fig. 4A, left) and a marked reduction in uptake of radioactivity after blocking (Fig. 4A, middle). The kinetics of radioactivity uptake are shown in the time–activity curves in Figure 4B. Uptake in nonblocked tumors increased rapidly during the first 30 min, followed by slower increases, with a tendency of leveling off at 50–60 min. Tumor uptake was

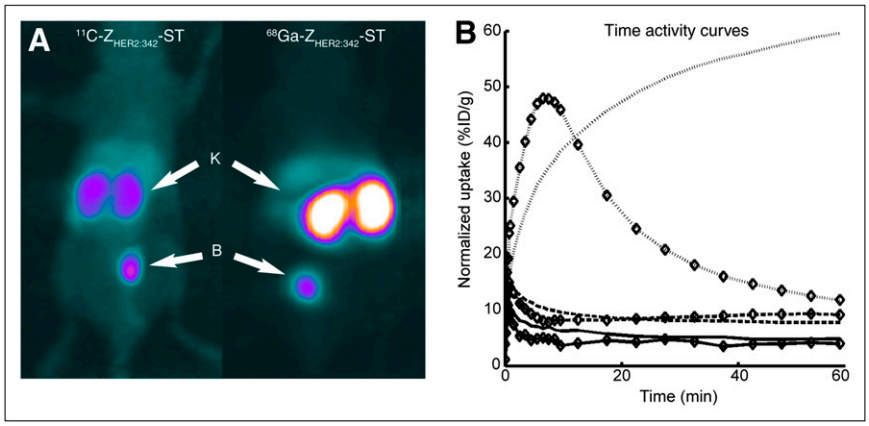

FIGURE 3. Biodistribution and pharmacokinetics of ^{11}C- and ^{68}Ga-labeled $Z_{HER2:342}$-ST. (A) Two representative maximum-intensity-projection PET images summed over 0–60 min of biodistribution of ^{11}C-$Z_{HER2:342}$-ST and ^{68}Ga-$Z_{HER2:342}$-ST-DOTA. Kidneys and bladder are indicated by arrows. (B) Time–activity curves for kinetics of ^{11}C-$Z_{HER2:342}$-ST (◇) and ^{68}Ga-$Z_{HER2:342}$-ST-DOTA (no symbol) in blood (solid line), kidneys (dotted line), and liver (dashed line). B = bladder; K = kidneys.

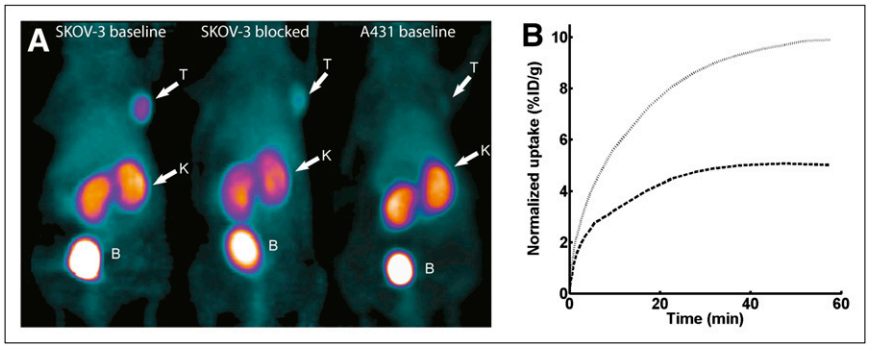

FIGURE 4. Tumor targeting and its specificity using ^{11}C-labeled $Z_{HER2:342}$-ST Affibody molecule. (A) Representative maximum-intensity-projection PET images summed over 10–60 min of tumor targeting using ^{11}C-$Z_{HER2:342}$-ST in mouse carrying HER2-expressing SKOV-3 xenograft, without blocking (left) and after blocking with excess of cold tracer (middle), and mouse carrying A431 tumor with low HER2 expression (right). Tumors, kidneys, and bladder are indicated by arrows. (B) Kinetics of tumor uptake in blocked (dashed) and nonblocked (dotted) tumors are presented in time–activity curves. Statistical parameters are presented in Figure 5. B = bladder; K = kidneys; T = tumors.

9.9 ± 1.8 %ID/g (n = 8) at 32.5 min. The biodistribution of ^{11}C-$Z_{HER2:342}$-ST in tumor-bearing mice was otherwise similar to that in non–tumor-bearing mice. After blocking with nonlabeled protein, uptake in the SKOV-3 tumors plateaued after approximately 30 min. Levels decreased significantly to 5.0 ± 1.3 %ID/g at 1 h (P = 0.002), indicating that the tumor uptake was HER2-mediated. The biodistribution in blocked and nonblocked animals was similar, apart from a slightly slower elimination of radioactivity to the urine observed in the second experiments, possibly due to insufficient rehydration between scans (Supplemental Fig. 1).

A significantly lower uptake of radioactivity was found in A431 xenografts than in the SKOV-3 tumors (P = 0.0001) (Fig. 4A, right) and at a level similar to that in the preblocked SKOV-3 tumors (Fig. 5). Immunohistochemistry staining confirmed high HER2 expression in the excised SKOV-3 tumors and moderate expression in the A431 tumors (Fig. 6).

DISCUSSION

The development of imaging methods for detecting HER2-overexpressing tumors could make considerable contributions to predicting the prognosis and stratification of patients for appropriate therapy (*3,4*). This study suggests that PET with ^{11}C-labeled HER2-targeting Affibody molecules may represent a promising step toward development of a method for specific, rapid, and repetitive monitoring over time of receptor expression levels in tumors.

In addition to their demonstrated high affinities to specific targets, the small size of the Affibody molecules gives them excellent pharmacokinetic properties, with rapid clearance from the blood and nontarget tissues, making tumor imaging on the day of injection possible (*18*). By ^{11}C labeling, dose exposures could be reduced and repeated investigations facilitated. It is known that the HER2-targeting Affibody molecule and the therapeutic monoclonal antibody trastuzumab bind distinct, nonoverlapping epitopes of HER2 (*18,31,32*). An attractive and important application of the Affibody-mediated HER2 imaging would be monitoring therapeutic responses to trastuzumab. The speed of the imaging described here and the lower doses from the ^{11}C-labeled radiotracer would likely allow for repeated imaging of such a therapeutic response. However, it was vital that the Sel-tagged Affibody molecules retained their expected cell-targeting specificities. As evaluated with fluorescence-activated cell sorting, using the tagged proteins fluorescently labeled with 5-IAF, we found that the C-terminal Sel-tag did not disturb the binding to their target receptors, a prerequisite for the in vivo imaging experiments.

It was an added advantage that the Sel-tag could be used to label $Z_{HER2:342}$ with either ^{11}C or ^{68}Ga for comparison of the impact of the radionuclide on imaging characteristics using the same ligand scaffold. Because of the short half-

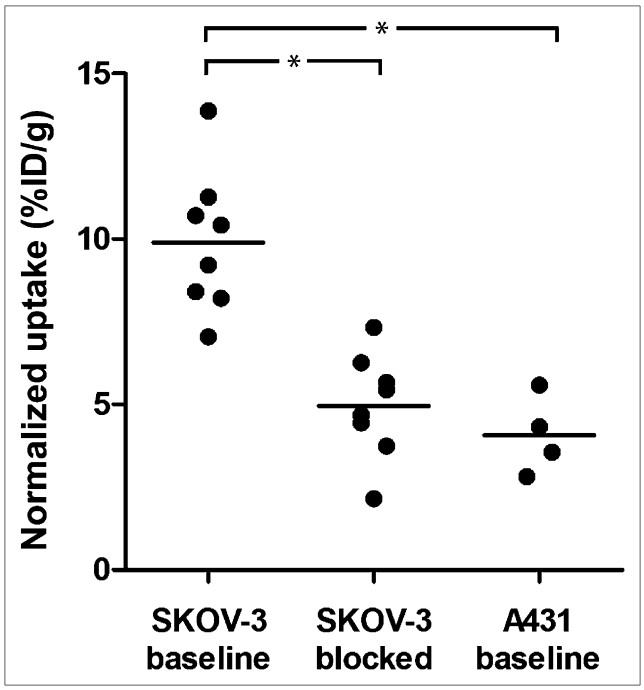

FIGURE 5. In vivo binding specificity of ^{11}C-$Z_{HER2:342}$-ST in mice carrying HER2-expressing SKOV-3 tumors and low-expressing A431 tumors. Tumor uptake of ^{11}C-$Z_{HER2:342}$-ST was significantly reduced (P = 0.002) after blocking of HER2 receptors with cold tracer and in tumors with low expression of HER2, compared with nonblocked SKOV-3 tumors. Tumor uptake at 32.5 min is presented. Significant reductions are marked with asterisks in the figure. *$P < 0.05$.

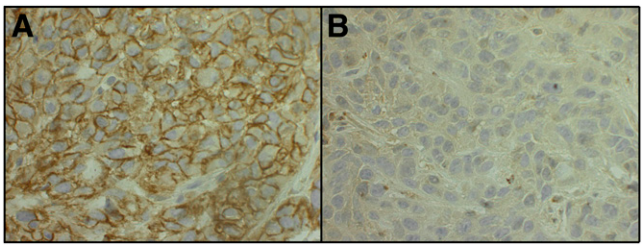

FIGURE 6. Immunohistochemical staining of HER2 in SKOV3 tumors (A) and A431 tumors (B). Images showed clear staining for HER2 localized to membrane in SKOV3 tumors, whereas HER2 expression in A431 tumors was considerably weaker.

life of ^{11}C, these comparisons could also be made in the same animals, further reducing interindividual bias. Both the ^{11}C- and the ^{68}Ga-labeled tracers displayed rapid initial and thereafter much slower clearance of remaining radioactivity from the blood. The main difference observed was the considerably higher retention of ^{68}Ga in the kidneys. High renal uptake is a common problem for many radiometal-labeled small proteins and peptides (*33*). Although this problem may be of less significance for detecting malignancies when, as in breast cancer, the kidneys are not a common metastatic site, high kidney uptake can potentially become dose-limiting for longitudinal monitoring of therapeutic effects. In sharp contrast to the ^{68}Ga-label, the ^{11}C radioactivity cleared much more rapidly from the kidneys. In fact, the radioactivity concentration and consequently the absorbed dose in the kidneys at the end of the scan were among the lowest reported for any HER2-binding Affibody molecule at that time point. The large difference in kidney uptake and retention obtained with the 2 tracers is most likely due to a high degree of reabsorption of the Affibody molecule from the primary urine in the proximal tubule (*34*) and subsequent intracellular degradation and trapping of the residualizing ^{68}Ga-label, whereas nonresidualizing ^{11}C is cleared quickly. The absorbed dose in all tissues will furthermore be lower because of the short half-life of ^{11}C. Furthermore, the lower energy of the positron emitted by ^{11}C than ^{68}Ga yields higher-resolution images, thereby improving detection of small lesions. These observations indicate that ^{11}C-labeled Affibody molecules have excellent imaging properties and may, in some settings, display advantages over probes labeled with residualizing radiometals.

The tumor-targeting capability of ^{11}C-$Z_{HER2:342}$-ST was clearly demonstrated in our experiments with mice with HER2-expressing xenografts. The tumor uptake of 10 %ID/g allowed unambiguous visualization of the tumors already after 30 min, suggesting that static imaging 30–40 min after injection could also be possible in clinical settings. However, uptake in tumors may also be due to unspecific uptake and retention effects. Here, because of the short half-life of ^{11}C, the specificity of tumor uptake could be probed in the same individual animals. The preadministration with excess unlabeled protein resulted in a significant reduction in tumor uptake in the second scan performed only 3 h later. Had the tumor uptake been largely affected by unspecific permeability and retention effects, which is often the case with larger molecules (*35*), this reduction in uptake would not have been expected. Moreover, the fact that the uptake was reduced in the blocking experiment to levels similar to those in A431 xenografts having low HER2 expression provided further evidence that the in vivo uptake of ^{11}C-$Z_{HER2:342}$-ST was rather specific for imaging of available HER2 receptors in the tumor tissue. Some uptake could be seen in both A431 tumors and in blocked SKOV-3 tumors. This uptake in both tumor types could potentially be due to a low level of HER2 expression in the A431 cells detectable by the high-affinity HER2 binder and an incomplete blockage of receptors in the SKOV-3 tumors with unlabeled tracer. However, the uptake could also be due to the permeability and retention effects, which could lead to a certain degree of unspecific uptake in tumors.

The choice of radionuclide is crucial for the utility of all in vivo radiotracers. With the rapidly expanding use of ^{18}F-FDG PET for detecting lesions with aberrant metabolic rates (*36*), the availability of PET centers with cyclotrons (and cyclotron-produced radionuclides) has increased, and clinical applications of positron-emitting nuclides have widened. Although longer-lived radionuclides such as ^{124}I and ^{89}Zr are being used to label slowly clearing antibodies and fragments (*37*), the shorter-lived ^{18}F and, as now shown here, even ^{11}C may be more appropriate choices for probes with rapid pharmacokinetics. Rapid radiolabeling procedures, such as the ^{11}C-labeling of the Sel-tag demonstrated here, are enabling technologies toward their implementation.

Future studies of interest include evaluation of the in vivo imaging potential of the ^{11}C-labeled, Sel-tagged EGFR-targeting Affibody molecule described here. Further elaboration of the HER2-targeting Affibody molecules' ability to detect fluctuation in HER2 expression, during disease development and during different therapeutic protocols, is highly warranted.

CONCLUSION

Affibody molecules could be Sel-tagged for site-specific labeling without loss of targeting ability. The favorable pharmacokinetics of the Affibody molecule in combination with the short-lived ^{11}C provided a radiotracer with improved characteristics for rapid and repeated imaging of HER2 levels.

DISCLOSURE STATEMENT

The costs of publication of this article were defrayed in part by the payment of page charges. Therefore, and solely to indicate this fact, this article is hereby marked "advertisement" in accordance with 18 USC section 1734.

ACKNOWLEDGMENTS

We thank Drs. Lars Abrahmsén, Joachim Feldwisch, Vladimir Tolmachev, Anna Orlova, and Johan Rockberg

for fruitful discussions and Daniel Rosik for technical assistance. We also thank the other members of the Sel-tag project—Hanna Lindberg, Filippa Fleetwood, Dr. John Löfblom, Professor Stig Linder, and Professor Sten Nilsson—for their input and further discussions. This work was supported by grants from the Swedish Foundation for Strategic Research (grant RBa08-0067), the Governmental Agency for Innovation Systems (grant 2009-00179), the Swedish Cancer Society (grants CAN 2010/691 and 2009/739), the Swedish Research Council (grants 40510402, 2004-5104, 2008-2654, and 2008-3186), and the Karolinska Institutet. No other potential conflict of interest relevant to this article was reported.

REFERENCES

1. Brufsky A. Trastuzumab-based therapy for patients with HER2-positive breast cancer: from early scientific development to foundation of care. *Am J Clin Oncol.* 2010;33:186–195.
2. O'Toole SA, Selinger CI, Millar EK, Lum T, Beith JM. Molecular assays in breast cancer pathology. *Pathology.* 2011;43:116–127.
3. Capala J, Bouchelouche K. Molecular imaging of HER2-positive breast cancer: a step toward an individualized 'image and treat' strategy. *Curr Opin Oncol.* 2010;22:559–566.
4. Oude Munnink TH, Nagengast WB, Brouwers AH, et al. Molecular imaging of breast cancer. *Breast.* 2009;18(suppl 3):S66–S73.
5. Dijkers EC, Oude Munnink TH, Kosterink JG, et al. Biodistribution of ^{89}Zr-trastuzumab and PET imaging of HER2-positive lesions in patients with metastatic breast cancer. *Clin Pharmacol Ther.* 2010;87:586–592.
6. Perik PJ, Lub-De Hooge MN, Gietema JA, et al. Indium-111-labeled trastuzumab scintigraphy in patients with human epidermal growth factor receptor 2-positive metastatic breast cancer. *J Clin Oncol.* 2006;24:2276–2282.
7. Serdons K, Verbruggen A, Bormans GM. Developing new molecular imaging probes for PET. *Methods.* 2009;48:104–111.
8. Tolmachev V, Stone-Elander S. Radiolabelled proteins for positron emission tomography: pros and cons of labelling methods. *Biochim Biophys Acta.* 2010; 1800:487–510.
9. Dimitrakopoulou-Strauss A, Strauss LG. PET imaging of prostate cancer with ^{11}C-acetate. *J Nucl Med.* 2003;44:556–558.
10. Singhal T, Narayanan TK, Jain V, Mukherjee J, Mantil J. ^{11}C-L-methionine positron emission tomography in the clinical management of cerebral gliomas. *Mol Imaging Biol.* 2008;10:1–18.
11. Cheng Q, Stone-Elander S, Arner ES. Tagging recombinant proteins with a Sel-tag for purification, labeling with electrophilic compounds or radiolabeling with ^{11}C. *Nat Protoc.* 2006;1:604–613.
12. Johansson L, Chen C, Thorell JO, et al. Exploiting the 21st amino acid-purifying and labeling proteins by selenolate targeting. *Nat Methods.* 2004;1:61–66.
13. Nord K, Gunneriusson E, Ringdahl J, Stahl S, Uhlen M, Nygren PA. Binding proteins selected from combinatorial libraries of an alpha-helical bacterial receptor domain. *Nat Biotechnol.* 1997;15:772–777.
14. Löfblom J, Feldwisch J, Tolmachev V, Carlsson J, Stahl S, Frejd FY. Affibody molecules: engineered proteins for therapeutic, diagnostic and biotechnological applications. *FEBS Lett.* 2010;584:2670–2680.
15. Schmidt MM, Wittrup KD. A modeling analysis of the effects of molecular size and binding affinity on tumor targeting. *Mol Cancer Ther.* 2009;8:2861–2871.
16. Orlova A, Magnusson M, Eriksson TL, et al. Tumor imaging using a picomolar affinity HER2 binding affibody molecule. *Cancer Res.* 2006;66:4339–4348.
17. Ahlgren S, Tolmachev V. Radionuclide molecular imaging using Affibody molecules. *Curr Pharm Biotechnol.* 2010;11:581–589.
18. Baum RP, Prasad V, Muller D, et al. Molecular imaging of HER2-expressing malignant tumors in breast cancer patients using synthetic ^{111}In- or ^{68}Ga-labeled affibody molecules. *J Nucl Med.* 2010;51:892–897.
19. Tolmachev V, Rosik D, Wallberg H, et al. Imaging of EGFR expression in murine xenografts using site-specifically labelled anti-EGFR ^{111}In-DOTA-Z EGFR:2377 Affibody molecule: aspect of the injected tracer amount. *Eur J Nucl Med Mol Imaging.* 2010;37:613–622.
20. Tolmachev V, Velikyan I, Sandstrom M, Orlova AA. HER2-binding Affibody molecule labelled with ^{68}Ga for PET imaging: direct in vivo comparison with the ^{111}In-labelled analogue. *Eur J Nucl Med Mol Imaging.* 2010;37:1356–1367.
21. Ahlgren S, Orlova A, Rosik D, et al. Evaluation of maleimide derivative of DOTA for site-specific labeling of recombinant affibody molecules. *Bioconjug Chem.* 2008;19:235–243.
22. Ahlgren S, Wallberg H, Tran TA, et al. Targeting of HER2-expressing tumors with a site-specifically ^{99}mTc-labeled recombinant affibody molecule, $Z_{HER2:2395}$, with C-terminally engineered cysteine. *J Nucl Med.* 2009;50:781–789.
23. Larsen P, Ulin J, Dahlstrøm K, Jensen M. Synthesis of [^{11}C]iodomethane by iodination of [^{11}C]methane. *Appl Radiat Isot.* 1997;48:153–157.
24. Tran TA, Rosik D, Abrahmsen L, et al. Design, synthesis and biological evaluation of a multifunctional HER2-specific Affibody molecule for molecular imaging. *Eur J Nucl Med Mol Imaging.* 2009;36:1864–1873.
25. Velikyan I, Maecke H, Langstrom B. Convenient preparation of ^{68}Ga-based PET-radiopharmaceuticals at room temperature. *Bioconjug Chem.* 2008;19:569–573.
26. Snyder WS, Ford MR, Warner GG, Watson SB. *"S," Absorbed Dose per Unit Cumulated Activity for Selected Radionuclides and Organs*. MIRD pamphlet 11. New York, NY: Society of Nuclear Medicine; 1975.
27. Xu X, Zhou Q, Korfmacher WA. Development of a low volume plasma sample precipitation procedure for liquid chromatography/tandem mass spectrometry assays used for drug discovery applications. *Rapid Commun Mass Spectrom.* 2005;19:2131–2136.
28. Fayad W, Brnjic S, Berglind D, et al. Restriction of cisplatin induction of acute apoptosis to a subpopulation of cells in a three-dimensional carcinoma culture model. *Int J Cancer.* 2009;125:2450–2455.
29. Tolmachev V, Wallberg H, Sandstrom M, Hansson M, Wennborg A, Orlova A. Optimal specific radioactivity of anti-HER2 Affibody molecules enables discrimination between xenografts with high and low HER2 expression levels. *Eur J Nucl Med Mol Imaging.* 2011;38:531–539.
30. Ekblad T, Tran T, Orlova A, et al. Development and preclinical characterisation of ^{99m}Tc-labelled Affibody molecules with reduced renal uptake. *Eur J Nucl Med Mol Imaging.* 2008;35:2245–2255.
31. Eigenbrot C, Ultsch M, Dubnovitsky A, Abrahmsen L, Hard T. Structural basis for high-affinity HER2 receptor binding by an engineered protein. *Proc Natl Acad Sci USA.* 2010;107:15039–15044.
32. Orlova A, Wallberg H, Stone-Elander S, Tolmachev V. On the selection of a tracer for PET imaging of HER2-expressing tumors: direct comparison of a ^{124}I-labeled affibody molecule and trastuzumab in a murine xenograft model. *J Nucl Med.* 2009;50:417–425.
33. Akizawa H, Uehara T, Arano Y. Renal uptake and metabolism of radiopharmaceuticals derived from peptides and proteins. *Adv Drug Deliv Rev.* 2008; 60:1319–1328.
34. Wållberg H, Orlova A, Altai M, et al. Molecular design and optimization of ^{99m}Tc-labeled recombinant Affibody molecules improves their biodistribution and imaging properties. *J Nucl Med.* 2011;52:461–469.
35. Iyer AK, Khaled G, Fang J, Maeda H. Exploiting the enhanced permeability and retention effect for tumor targeting. *Drug Discov Today.* 2006;11:812–818.
36. Zhu A, Lee D, Shim H. Metabolic positron emission tomography imaging in cancer detection and therapy response. *Semin Oncol.* 2011;38:55–69.
37. van Dongen GA, Vosjan MJ. Immuno-positron emission tomography: shedding light on clinical antibody therapy. *Cancer Biother Radiopharm.* 2010;25:375–385.